

SUPPORTING INFORMATION

Interaction of an Antimicrobial Peptide with a Model Lipid Bilayer using Molecular Dynamics Simulation

Wael Soliman,[‡] Subir Bhattacharjee,[†] Kamaljit Kaur^{‡,}*

Methods

Peptide Structure

CbnB2 is a 48-residue cationic antimicrobial peptide with a net charge of +4 at neutral pH. It forms a stable secondary structure in 2,2,2-trifluoroethanol or detergent micelles but is essentially unstructured in water as shown by NMR and MD simulations studies.^{1, 2} CbnB2 folds into a well-defined central helical structure (residues 18-39) and disordered N and C termini forming mainly a coil structure. The N-terminus contains a conserved disulfide bond between Cys9 and Cys14. The α -helical wheel representation of residues 18-39 of CbnB2 shows that the peptide is amphipathic with a polar/hydrophilic and hydrophobic face as shown in Figure S1. This is further supported by the high amphipathicity value of 4.24 for the helix. Amphipathicity was determined by the calculation of hydrophobic moment ³ of the helical residues using the software package JEMBOSS version 1.5.⁴ The

three dimensional coordinates based on NMR solution structure of CbnB2 were obtained from the protein data bank, PDB code 1CW5.⁵ The starting structure of CbnB2 used in this study corresponds to the solution structure of CbnB2 (pdb code 1CW5) in TFE-*d*₃/H₂O (9:1) ~ pH 2.8⁵. The peptide was considered to have positively and negatively charged N-terminal NH₃⁺ and C-terminal COO⁻ groups, respectively. Lys, Arg, and Glu residues were considered to be charged, and His residue was kept neutral giving CbnB2 a charge of +4.

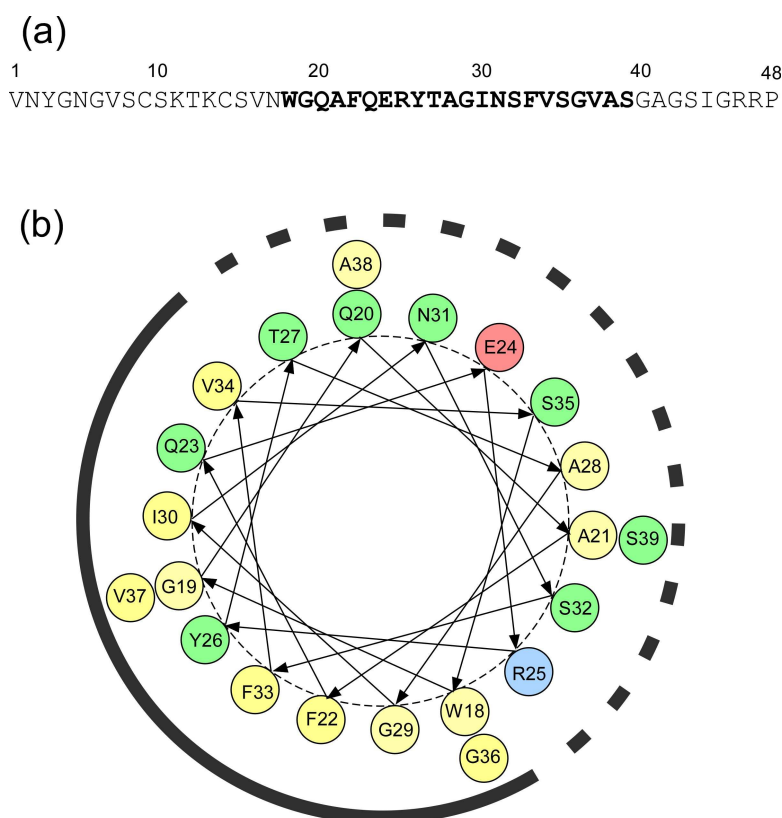


Figure S1. (a) Amino acid sequence of CbnB2. The helical residues (18-39) are in bold. (b) Edmundson α -helical wheel representation of residues 18-39 of CbnB2. The solid curve indicates the hydrophobic face and the dashed curve denotes polar/hydrophilic face.

Simulation Box Construction

A lipid bilayer made of POPG and POPE (Figure S2) homogenously distributed in a bilayer structure (75 per leaflet) was used to mimic the cell membranes of gram-positive bacteria. The analysis of major phospholipid components of several gram positive bacteria show that they contain mostly PG and PE lipids with the former reaching up to 80%.⁶⁻⁸ The PDB coordinates for the POPG and POPE molecules were obtained from http://moose.bio.ucalgary.ca/login.ezproxy.library.ualberta.ca/index.php_page=Structures_and_Topologies⁹ and <http://www.wellesley.edu/Chemistry/Don/download.html>¹⁰, respectively.

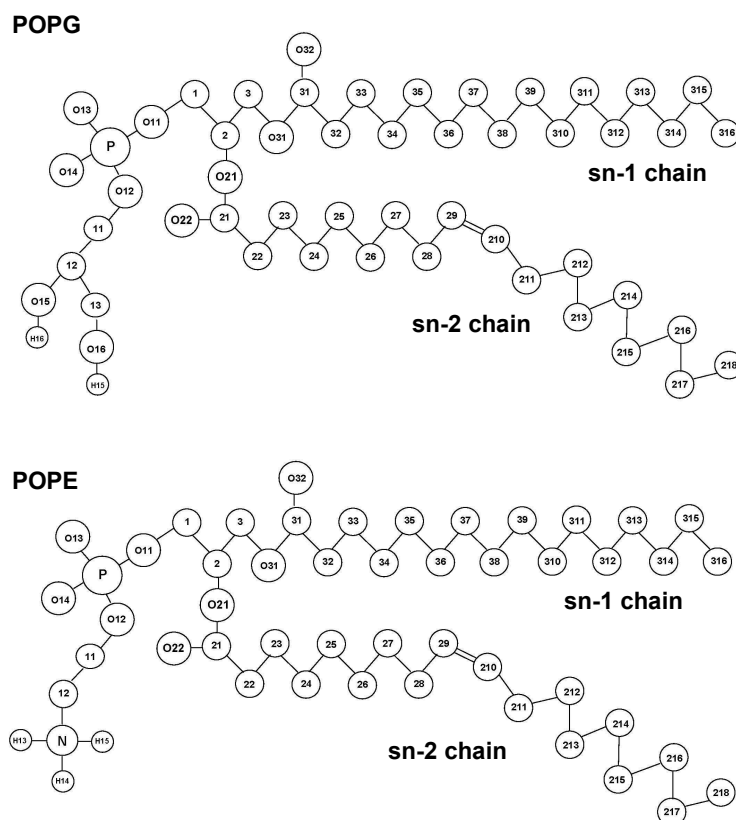


Figure S2. Schematic representation of the POPG and POPE showing the bond connections.

The system was set up by placing CbnB2 in three different positions (as described in the main text) with respect to the bilayer in a rectangular box. For simulations HI and I, CbnB2 was inserted in the bilayer by removing lipid molecules with phosphate atoms within 2.5 nm from any atom of CbnB2. The lipids molecules removed were later added to the bilayer on the sides. The starting configurations were generated by adding SPC water molecules on either side of the bilayer. Sufficient counterions (Na^+) were added to make the system electroneutral. Following this, 7 ions of Na^+ and Cl^- each were added to the simulation box to yield an excess background electrolyte concentration of 25 mM.^{11, 12} A simulation (simulation C) of lipid bilayer without the peptide was also run. For simulation HI-m, peptide was placed in the same orientation as in simulation HI and a single mutation at F33 (F33→S33) was introduced. The details of the periodic cell for each system, including the number of water molecules, lipids, and the initial box size, are listed in Table S1.

Table S1: Details of MD simulations in the NPT ensemble

Simulation	No. of atoms	No. of water molecules	No. of lipids		Initial box size (nm)
			POPG	POPE	
C	40548	10851	112	38	6.8 x 6.8 x 10
S	41016	10856	112	38	7 x 7 x 10
HI	40977	10843	112	38	7 x 7 x 10
I	40995	10849	112	38	7 x 7 x 10
HI-m	40992	10851	112	38	7 x 7 x 10

Simulation Methods and Parameters

MD simulations were performed using the GROMACS 3.33 simulation package and the GROMOS96 force field on a four node cluster.^{13, 14} All systems were simulated in the isobaric-isothermal (NPT) ensemble at 300 K using periodic boundary conditions. Weak coupling of the

proteins to a solvent bath of constant temperature was maintained using the Berendsen thermostat with a coupling constant $\tau_T = 0.1$ ps. The pressure was controlled using the Berendsen algorithm at 1 bar with a coupling constant $\tau_P = 1$ ps at 300 K. For all simulations, the neighbor list was updated every 10 steps, with a neighbor list cut-off distance of 1.2 nm. The Lennard-Jones interactions were truncated at a cutoff distance of 1.2 nm. The long-range electrostatic interactions were modeled using the particle mesh Ewald (PME) summation method with a cutoff distance of 1.2 nm for the real space. The integration time step was 2 fs, and the coordinates and velocities were saved every 4 ps. The LINCS algorithm was used to restrain all bond lengths.¹⁵ The system was energy minimized before the MD simulation using 1000 steps of the steepest descent energy minimization method in order to relax any steric conflicts generated during the set-up. The equilibration of the CbnB2-bilayer–water system was achieved by performing a 5 ns MD run with positional restraint on the peptide. Following this, a full MD run of 50 ns were performed without any restraints. Simulations were analyzed using various GROMACS postprocessing routines. Swiss-PdbViewer¹⁶ and ViewerLite 5.0¹⁷ were used to visualize and superimpose structures.

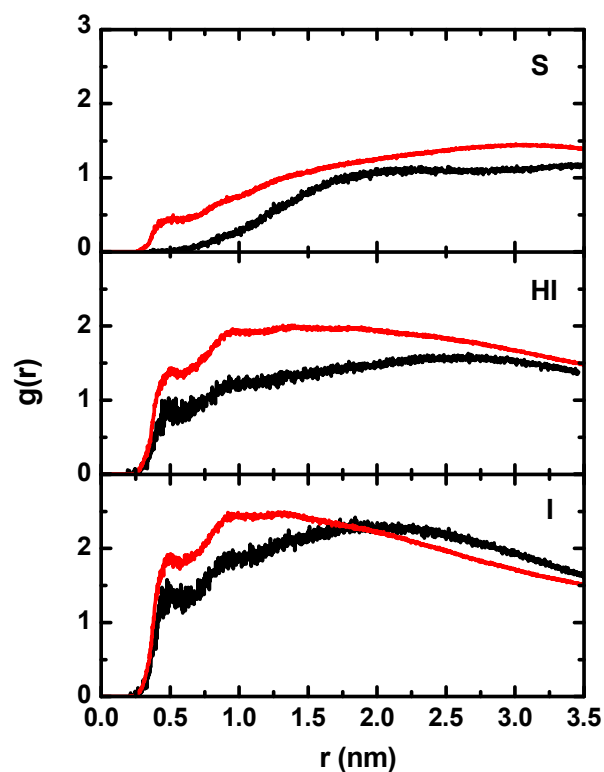


Figure S3. Radial distribution functions $g_{\text{lipid tail-helix}}$ for simulations S, HI, and I. The lipid tail refers to the alkyl chains of the lipid molecule and helix refers to the helical region of CbnB2 (residues 19-40). The average is between 0-1 ns (black) and 45-50 ns (red) for all the simulations.

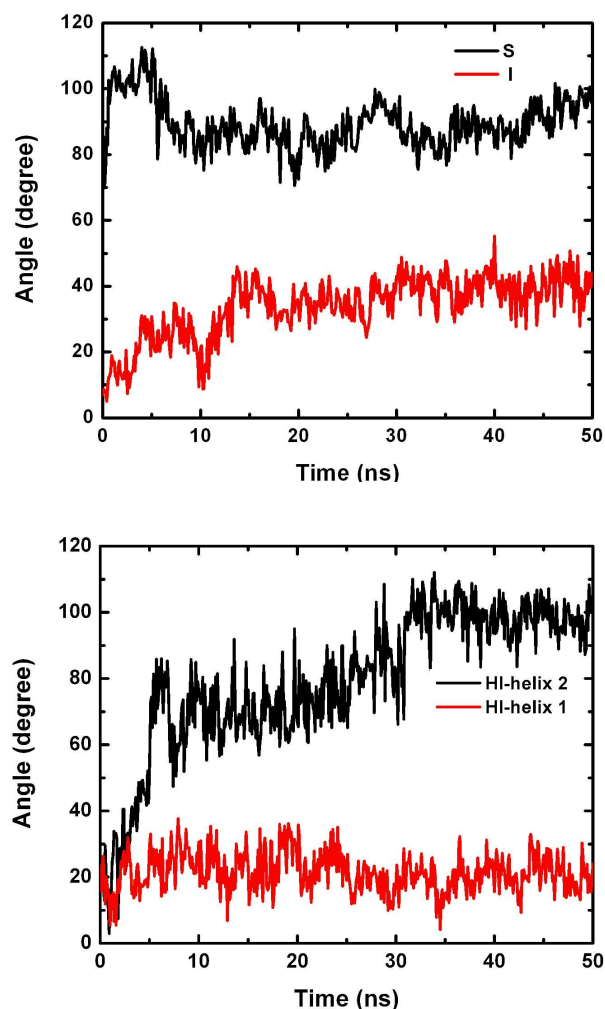


Figure S4. Angle between the helical region of CbnB2 and the lipid bilayer showing the orientation of peptide with respect to bilayer during simulations S, HI, and I. For simulation S and I, the angle is calculated between a vector passing through the C α of N31 and S35 (helical region) and z axis of the bilayer. The helical region in simulation HI is interrupted by a hinge region to give helix 1 (residue 19-32) and helix 2 (residues 37-41). The angle for simulation HI is calculated using two vectors, one passing through the C α of V26 and A30 (helix 1) and the other passing through the C α of A38 and S39 (helix 2). The angle shown is between helix 1 and bilayer z-axis (red) as well as helix 2 and bilayer z-axis (black).

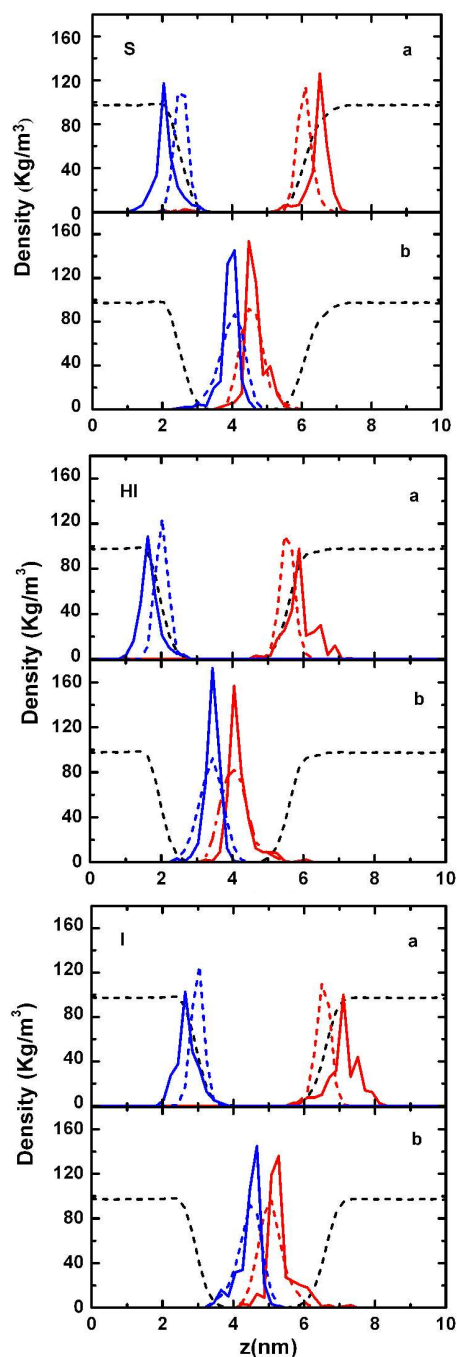


Figure S5. Density profiles of phosphorous (a) and the lipid tails (b) of the lipid molecules and water for simulations S, HI and I. Red, blue, and black lines correspond to from the upper leaflet, lower leaflet of the bilayer, and water. Densities are averaged for the first 1 ns (solid) and the last 10 ns (dot). Lipid tail density is calculated based on the densities of the three terminal methylene carbons (C215-217) from one of the alkyl chains of the lipid molecule. The density of water is divided by 10 to fit the scale. The distance is calculated along z direction (Fig. 1) from the bottom of the simulation box.

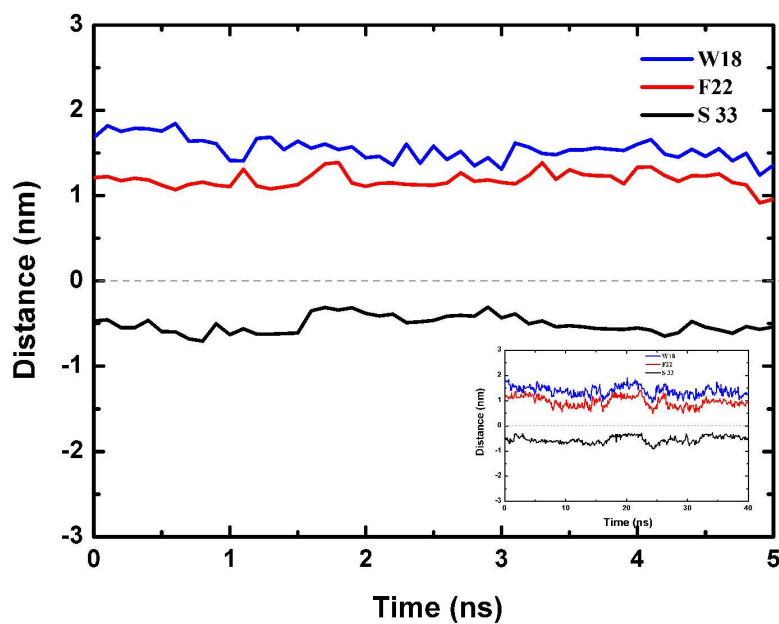


Figure S6. The distance between the centre-of-mass of the three hydrophobic residues of CbnB2 and phosphorous atoms of the top bilayer leaflet during simulation HI-m; W18 (blue), F22 (red), S33 (black), inset: distance during the entire simulation (0-50 ns). The position of the three residues, namely, W18, F22, and S33 did not change during the simulation.

References

1. Kaur, K.; Andrew, L. C.; Wishart, D. S.; Vederas, J. C., Dynamic relationships among type IIa bacteriocins: temperature effects on antimicrobial activity and on structure of the C-terminal amphipathic alpha helix as a receptor-binding region. *Biochemistry* **2004**, 43, (28), 9009-20.
2. Sailer, M.; Helms, G. L.; Henkel, T.; Niemczura, W. P.; Stiles, M. E.; Vederas, J. C., ¹⁵N- and ¹³C-labeled media from *Anabaena* sp. for universal isotopic labeling of bacteriocins: NMR resonance assignments of leucocin A from *Leuconostoc gelidum* and nisin A from *Lactococcus lactis*. *Biochemistry* **1993**, 32, (1), 310-8.
3. Eisenberg, D.; Weiss, R. M.; Terwilliger, T. C., The helical hydrophobic moment: a measure of the amphiphilicity of a helix. *Nature* **1982**, 299, (5881), 371-4.
4. Carver, T.; Bleasby, A., The design of Jemboss: a graphical user interface to EMBOSS. *Bioinformatics* **2003**, 19, (14), 1837-43.
5. Wang, Y.; Henz, M. E.; Gallagher, N. L.; Chai, S.; Gibbs, A. C.; Yan, L. Z.; Stiles, M. E.; Wishart, D. S.; Vederas, J. C., Solution structure of carnobacteriocin B2 and implications for structure-activity relationships among type IIa bacteriocins from lactic acid bacteria. *Biochemistry* **1999**, 38, (47), 15438-47.
6. Epand, R. F.; Savage, P. B.; Epand, R. M., Bacterial lipid composition and the antimicrobial efficacy of cationic steroid compounds (Ceragenins). *Biochim Biophys Acta* **2007**, 1768, (10), 2500-9.
7. Epand, R. F.; Schmitt, M. A.; Gellman, S. H.; Epand, R. M., Role of membrane lipids in the mechanism of bacterial species selective toxicity by two alpha/beta-antimicrobial peptides. *Biochim Biophys Acta* **2006**, 1758, (9), 1343-50.
8. Zhao, W.; Rog, T.; Gurtovenko, A. A.; Vattulainen, I.; Karttunen, M., Atomic-scale structure and electrostatics of anionic palmitoyloleoylphosphatidylglycerol lipid bilayers with Na⁺ counterions. *Biophys J* **2007**, 92, (4), 1114-24.
9. Tieleman, D. P.; Forrest, L. R.; Sansom, M. S.; Berendsen, H. J., Lipid properties and the orientation of aromatic residues in OmpF, influenza M2, and alamethicin systems: molecular dynamics simulations. *Biochemistry* **1998**, 37, (50), 17554-61.
10. Elmore, D. E., Molecular dynamics simulation of a phosphatidylglycerol membrane. *FEBS Lett* **2006**, 580, (1), 144-8.

11. Boziaris, I. S.; Skandamis, P. N.; Anastasiadi, M.; Nychas, G. J., Effect of NaCl and KCl on fate and growth/no growth interfaces of *Listeria monocytogenes* Scott A at different pH and nisin concentrations. *J Appl Microbiol* **2007**, 102, (3), 796-805.
12. Delgado, A.; Arroyo Lopez, F. N.; Brito, D.; Peres, C.; Fevereiro, P.; Garrido-Fernandez, A., Optimum bacteriocin production by *Lactobacillus plantarum* 17.2b requires absence of NaCl and apparently follows a mixed metabolite kinetics. *J Biotechnol* **2007**, 130, (2), 193-201.
13. Lindahl, E.; Hess, B.; van der Spoel, D., Gromacs 3.0: A package for molecular simulation and trajectory analysis. *J. Mol. Mod.* **2001**, 7, 306-317.
14. Spoel, D. V.; vanBuuren, A. R.; Apol, E.; Meulenhoff, P. J.; Tieleman, D. P.; Sijbers, A. L. T. M.; Hess, B.; Feenstra, K. A.; Lindahl, E.; vanDrunen, R.; Berendsen, H. J. C., *Gromacs User Manual Version 3.1.1*. Nijenborgh4, 9747 AG Groningen, The Netherlands. Internet: www.gromacs.org, 2002.
15. Hess, B.; Bekker, H.; Berendsen, H. J. C.; Fraaije, J., LINCS: A linear constraint solver for molecular simulations. *J. Comp. Chem.* **1997**, 18, (12), 1463-1472.
16. Guex, N.; Peitsch, M. C., SWISS-MODEL and the Swiss-PdbViewer: An environment for comparative protein modeling. *Electrophoresis* **1997**, 18, (15), 2714-2723.
17. MSI *WebLab ViewerLite Version 3.2*, Molecular Simulations Inc.: UK, (<http://molsim.vei.co.uk/weblab/>), 1998.